NASA TECHNICAL MEMORANDUM 102636

THREE-DIMENSIONAL ELASTIC-PLASTIC ANALYSIS OF SHALLOW CRACKS IN SINGLE-EDGE-CRACK-TENSION SPECIMENS

Kunigal N. Shivakumar and
James C. Newman, Jr.

April 1990

National Aeronautics and
Space Administration

Langley Research Center
Hampton, Virginia 23665

THREE-DIMENSIONAL ELASTIC-PLASTIC ANALYSIS OF SHALLOW CRACKS IN SINGLE-EDGE-CRACK-TENSION SPECIMENS

SUMMARY

Three-dimensional, elastic-plastic, finite-element results are presented for single-edge-crack-tension specimens with several shallow crack-length-to-width ratios ($0.05 \leq a/W \leq 0.5$). Results showed the need to model the initial yield plateau in the stress-strain behavior to accurately model deformation of the A36 steel specimens. The crack-tip-opening-displacement was found to be linearly proportional to the crack-mouth-opening displacement. A new deformation dependent η_p (plastic-eta factor) equation is presented for calculating the J-integral from test load-displacement records. This equation was shown to be accurate for all crack lengths considered.

1. INTRODUCTION

Damage tolerant design of welded joints in nuclear reactors and launch vehicles requires a nonlinear fracture mechanics parameter like J because the materials used are highly ductile. Cracks in these structural components are typically shallow. The J-integral data for shallow cracks and simplified calculation methods are limited or not available. However, a wealth of experimental data and accurate simplified techniques are reported in the literature for deep cracks [1 - 6] in ductile materials. The difficulty in developing simplified J-integral techniques for shallow cracks is due to the interaction of tension and bending deformations in addition to the material nonlinearity. Recognizing the importance of developing shallow-crack test methodology, *The International Research Project to Develop Shallow Crack Fracture Mechanics Tests* was initiated jointly by The Welding Institute (UK) and The Edison Welding Institute (USA). Government laboratories and industries in the United States and Europe participated in this program. As a part of this study, NASA Langley Research Center conducted three-dimensional (3D), elastic-plastic, finite-element (FE) analyses of single-edge-crack-tension, SE(T)[1], specimens.

The objectives of this paper are: (1) to present results of three-dimensional, elastic-plastic, finite-element analyses of SE(T) specimens for crack-length-to-width (a/W) ratios ranging

---

[1]ASTM notation for single-edge-crack-tension specimen.

from 0.05 to 0.5; and (2) to develop a simplified method to evaluate the J-integral for shallow cracks using the measured load and load-line displacement. The load-line displacements, crack-mouth-opening displacements (CMOD), and crack-tip-opening displacements (CTOD) are evaluated and are compared with each other. The equivalent domain integral method [7-9] is used to evaluate the J-integral along the crack front. A dimensional analysis, similar to that used by Rice et.al.[1], Paris et. al.[2], and Ernst[5], is used to develop a deformation dependent plastic-eta (η_p) factor. This η_p factor can be used to evaluate J from the measured load, load-line displacement, and material properties.

2. SPECIMEN AND MATERIAL PROPERTIES

Figure 1(a) shows the SE(T) specimen configuration and loading P. The specimen width is W (25 mm), thickness is B (25 mm), and the crack length is a. The specimen total length is 450 mm and the length between the load points is 350 mm. The load-line displacement is computed at gage points located under the load (mid-width) and 100 mm (L) apart (see Fig. 1(a)). Symmetry of the specimen configuration and loading allows one to model only one-quarter of the specimen in the F-E analysis. Six crack configurations were considered: a/w = 0.5, 0.4, 0.3, 0.2, 0.1, and 0.05. The material used was an A36 steel with E = 207 kN/mm^2, Poisson's ratio ν = 0.3, yield stress σ_y = 283.4 N/mm^2, and ultimate tensile strength σ_u = 470 N/mm^2. This material was

used in the international test program mentioned previously. Like many other steels, this material also exhibited an initial yield plateau at σ_y = 283.4 N/mm^2 (see Fig. 1(b)). The complete uniaxial stress-strain response was represented by a piecewise linear approximation as shown by the straight line segments in the figure. Figure 1(b) also defines a secant modulus E_s corresponding to a nominal tensile strain of ϵ_n.

3. FINITE-ELEMENT ANALYSIS

A three-dimensional, elastic-plastic, finite-element program, developed in-house at NASA Langley Research Center [10], was used in this study. The program was developed using 8-noded hexahedron elements, von Mises yield criterion, isotropic hardening, small strain deformation theory, and associated flow rule. The numerical algorithm was based on the initial-stress method and incremental theory of plasticity. The material stress-strain characteristics can be elastic-perfectly plastic, Ramberg-Osgood, or multilinear type. The program has special features like modelling crack extension and an option to use reduced shear-integration for bending dominant problems. The program includes the J-integral evaluation by the equivalent domain integral method [7-9].

The 3D finite-element meshes were generated by translating the two-dimensional (2D) mesh (for example, shown in Fig. 2) in the z-direction. The present study involved analyses of several crack configurations with the other geometric parameters

remaining constant; hence, a simplified mesh generation scheme was adopted. In this scheme, a fine polar mesh around the crack front was developed separately (Region A). An array of rectangular and triangular elements was used to idealize the specimen elsewhere. Figure 2 shows a typical 2D idealization of the specimen for $a/W = 0.3$. Region A represents the mesh refinement around the crack front. For $a/W \geq 0.1$, the mesh pattern was obtained by changing the location of region A within region B. For $a/W = 0.05$, the element sizes in region A were reduced to one-half of that used for the other cases and the remaining region was proportionately scaled to make up the total width. In all models, the crack tip had multiple nodes. The element nodes at the crack tip all had the same coordinates but with different node numbers. The twelve elements around the crack tip lead to thirteen different nodes at the crack tip and only the node for the right most element was restrained from deforming. Such an arrangement would give the local CTOD by blunting the crack tip during plastic deformation [11].

The 3D mesh had five layers, with layer thicknesses of 6, 3, 2, 1, and 0.5 mm. The smallest layer was located at the free surface of the specimen. The model had 1680 nodes and 1220 elements. The elastic-plastic analysis was performed by incrementing the displacements applied at the load points shown in the Fig. 1(a). The displacement increment selected was twenty percent of the initial yield displacement. The analysis was terminated when the CMOD $\geq$ 1 mm, CTOD $\geq$ 0.5 mm, or the program

exceeded the specified time limit (25,000 CRUs in CDC 205 computer). In calculating the J-integral, several domains around the crack front were used but they were found to give the nearly the same values. Hence, J-values from only the domain shown in Figure 2 at six nodal locations along the crack front are presented.

4. EQUIVALENT DOMAIN INTEGRAL METHOD

The total J-integral at any point along the crack front in a 3D cracked body is defined as an integral over a closed surface around the crack front (The tube represented by the broken line in Fig. 3) as [12]

$$J = \lim_{\substack{r/\Delta \to 0 \\ \Delta \to 0}} \frac{1}{\Delta} \int_{A_r + O_1 + O_2} \left(w\, n_1 - \sigma_{ij} \frac{\partial u_i}{\partial x_1} n_j \right) dA \qquad (1)$$

where w is the stress work density, defined as

$$w = \int_0^{\epsilon_{ij}} \sigma_{ij}\, d\epsilon_{ij} \qquad (2)$$

In Eq. 1, σ_{ij} and ϵ_{ij} are stress and strain tensors on the surface of the tube, u_i is the displacement vector, n_j is the jth component of the unit normal vector on the surface, Δ is the projected length of the crack front along the x_3 axis, and

r is the radius of the tube over which the integral is evaluated. The indices i and j take the values 1, 2, and 3. Recently, the surface integral Eq. 1 was modified to a volume integral, called the equivalent domain integral [7-9], for ease of implementation in a finite-element analysis and accurate evaluation of the integral. This was accomplished by the application of Green's divergence theorem and de Lorenzi's [13] s-function. For traction-free crack faces, Eq. 1 is written as a volume integral between the inner tube A_r (broken line) and any other closed tube (solid line) enclosing A_r (see Fig. 3).

$$J = -\frac{1}{f}\left[\int\left[w\frac{\partial s}{\partial x}_1 - \sigma_{ij}\frac{\partial u_1}{\partial x_1}\frac{\partial s}{\partial x_j}\right]dv + \int\left[\frac{\partial w}{\partial x_1} - \sigma_{ij}\frac{\partial \epsilon_{ij}}{\partial x_1}\right]s\,dv\right] \qquad (3)$$

where s is any arbitrary but continuous function with a characteristic value of one on the inner tube and zero on all outer surfaces, and f is the integrated value of s along the x_3-axis. In the FE analysis, the volume integral was performed on one-ring of elements surrounding the crack front (see shaded area in Region A in Fig. 2) and one (for outer surfaces) or two (for interior region) layers of elements along the crack front. Equation 3 can be used for isotropic or anisotropic as well as linear or nonlinear materials. In the present incremental

elastic-plastic analysis, the stress work density, strains, and stresses were evaluated at each load step. Then, the J-integral was evaluated at specified load steps from the accumulated stress work density, total strain, stress, and displacement fields.

5. RESULTS AND DISCUSSIONS

Three-dimensional, elastic-plastic, finite-element analyses of SE(T) specimens for a/W ratios of 0.5, 0.4, 0.3, 0.2, 0.1, and 0.05 were performed. At each applied displacement, the load P, load-line displacement d_{ll}, crack-mouth-opening displacement (CMOD), crack-tip-opening displacement (CTOD), and the J-integral were evaluated. The CTOD was calculated by Tracey's 90 deg intercept method [11].

Figure 4 shows the normalized load (P/WB) against the load-line displacement (d_{ll}) for all six a/w ratios. Although the maximum d_{ll} for a/W ratios of 0.2, 0.1, and 0.05 were larger than 1.0 mm, curves are terminated at 1.0 mm for clarity. Load and load-line displacement curves for $a/W \leq 0.2$ show a sharp knee, whereas, the curves for $a/W \geq 0.3$ are smooth and similar in shape. The sharp knee in the load against load-line displacement curve is attributed to the initial yield plateau in the material stress-strain curve (see Fig.1(b)). The specimens for $a/W \leq 0.2$ have a dominant tension stress component compared to the bending stress component, unlike the cases of $a/W \geq 0.3$. Therefore, to predict the true response of shallow cracked tension specimens, modelling of the initial yield plateau of

stress-strain curve is important.

Figure 5 shows the plastic components of CTOD ($CTOD_p$) against CMOD ($CMOD_p$) at the midsection (z=0) of the specimen for a/W ratios of 0.5, 0.3, and 0.1. Results for other a/W ratios are a subset of those shown in the figure. After a small initial deformation ($CMOD_p \geq 0.1$ mm), the $CTOD_p$ varied linearly with $CMOD_p$. The same linearity was found between the total CTOD and CMOD (results are not shown), but with a slope smaller than that for plastic components.

Figure 6 shows the distribution of normalized J (EDI method) along the crack front for the three a/W ratios. J for each case is normalized by the J-value at the midsection (z = 0). Solid curves represent the elastic solution and the dashed curves represent the elastic-plastic solution at their respective plane stress limit load (plastic hinge condition). The limit load was $P_{ll} = (2\alpha - 1)bB\sigma_o$, where b is the uncracked ligament length (W - a), $\sigma_o = (\sigma_y + \sigma_u)/2$, and the term αb represents the distance of neutral axis (NA) from the crack tip (see Fig. 7). The equation for α is

$$\alpha = 1/2 \left[1 - a/b + \sqrt{(1 + (a/b)^2)} \right] \qquad (4)$$

The limit loads for a/W ratios of 0.5, 0.3, and 0.1 were 48.76 kN, 108.67 kN, and 189.65 kN, respectively, and the corresponding midsection J-values were 12.0 N/mm, 16.27 N/mm, and 90.73 N/mm. The elastic solution for all three curves show that J drops

near the free surface ($z = B/2$) due to the free-surface boundary-layer effect caused by the material Poisson's ratio [14, 15]. The relative drop off is more for deep crack (like $a/W = 0.5$) than for shallow crack (like $a/W = 0.1$) specimens. This is attributed to the larger anticlastic bending curvature in deep crack specimens compared to the shallow crack, as explained by Crews et al. [16]. For $a/W = 0.1$, the maximum J is not at the mid-section but at $z/B = 0.44$ for the elastic case and $z/B = 0.33$ for the elastic-plastic case. The variation of J along the crack front at the limit load condition is the same as that for the elastic case, except that the variation near the free surface is more pronounced.

Figure 8 shows the average J along the crack front plotted against the load-line displacement for several a/W ratios. Solid curves are from the EDI method and the dashed curves are from the J equation developed in the next section. $J - d_{11}$ curves for a/W ratios of 0.5 and 0.3 show a steep slope and fall nearly together. However, for $a/W < 0.3$ the J curves show a change in the curvature from concave to convex (through an inflection point). The characteristic change in the shape of the $J - d_{11}$ curve is believed to be related to initial yield plateau, subsequent hardening in the material stress-strain curve, and global tensile yielding (influences d_{11}) of the specimen. The J value, however, calculated by the EDI method is a local crack-tip parameter and is not affected by the global yielding.

6. DEFORMATION DEPENDENT PLASTIC ETA-FACTOR (η_p)

As explained in references 1-6, eta-factors greatly simplify the evaluation of G for linear-elastic materials and J for elastic-plastic materials in both test specimens and structural components. The simplicity is because only the measured load and the load-line displacement are used to compute G or J. For linear-elastic materials, the eta-factor can be shown to be dependent only on the specimen configuration (for example, see Ref. 6). This eta-factor is similar to the compliance derivative term in the usual G equation, hence it is only a configuration parameter. In general, for elastic-plastic materials, the eta-factor depends on the magnitude of deformation in addition to configuration. However, for deeply cracked (bending dominant) specimens, made of either power-law hardening nonlinear material [1] or elastic-plastic material the eta-factor was shown to be independent of deformation [1-5]. The present analysis was focused on developing a deformation dependent elastic-plastic eta-factor (η_p) for SE(T) specimens which is valid for a complete range of a/W ratios (shallow to deep). Dimensional analysis, like that in references 1, 2, and 5, was used to develop an equation for the η_p.

Following the energy method, the total J can be defined as the sum of the elastic (J_e) and the plastic (J_p) components. J_e is calculated from the stress-intensity-factor (K) for a given a/W ratio [17] using the standard linear elastic fracture mechanics relationship ($J_e = K^2 (1-\nu^2)/E$). The plastic component

J_p is defined as a differential of the plastic potential energy (W_p) with reference to the uncracked ligament, b ($J_p = 1/B\ (\partial W_p/\partial b)$). Under constant displacement conditions, J_p is written in terms of the load P and the plastic component of the load-line displacement d_{llp} as

$$J_p = \frac{1}{WB} \int_0^{d_{llp}} \frac{\partial P}{\partial (b/W)}\, d(d_{llp}) \qquad (5)$$

The load P is a function of the load-line displacement, material properties, crack length, and other configuration parameters of the specimen. Paris et al. [2] and Ernst [5] showed that for deeply cracked specimens, P can be expressed as a product of two functions where one is independent of deformation and the other independent of crack length. Thus, a plastic eta-factor (η'_p) can be defined which is constant for all deformations. Using these assumptions, Eq. 5 can be reduced to

$$J_p = \frac{\eta'_p}{bB} \int_0^{d_{llp}} P\, d(d_{llp}) \qquad (6)$$

Therefore, J_p and hence, J, can be calculated from the measured load and load-line displacements. If the assumption leading to Eq. 6 is valid, then the load and load-line displacement (total

or plastic component) curves for different a/W ratios would be in constant ratio to each other. The curves in figure 4 for a/W ratio of 0.4 and 0.5 in figure 4 show such a trend. Hence, η'_p can be found. However, the curves for $a/W < 0.3$ do not show such a trend and the curve for $a/W = 0.3$ falls in a transition region. Therefore, a new plastic eta-factor needs to be defined which would be valid for both deep and shallow cracks. Consider the load P as a product of two functions. One depends on crack length and deformation; the second is independent of crack length but depends on other configuration parameters and deformation. Therefore,

$$P = F(b/W,\ d_{11}/L)\quad H(d_{11}/L,\ B/W,\ \ldots) \qquad (7)$$

Then, one can show that

$$\frac{\partial P}{\partial (b/W)} = P \left\{ \frac{1}{F} \frac{\partial F}{\partial (b/W)} \right\} \qquad (8)$$

Substituting Eq. (8) in Eq. (5), J_p is written in terms of a deformation dependent plastic eta-factor (η_p) as

$$J_p = \frac{\eta_p}{bB} \int_0^{d_{11p}} P\, d(d_{11p}) \qquad (9)$$

Where

$$\eta_p = \frac{b}{WF}\left(\frac{\partial F}{\partial (b/W)}\right) \qquad (10)$$

This η_p is a function of d_{11}/L (ratio of load-line displacement to gage length L) and b/W. For shallow crack SE(T) specimens, the tension component of load-line displacement (d_{11t}) is more dominant than the bending component. Furthermore, for bending dominant deep crack specimens, η_p should become deformation independent [2-5]. Therefore, only d_{11t} (which is small or zero for deep cracks) is believed to introduce the deformation dependency to η_p factor. Therefore η_p in Eq. 10 can be expressed as a function of tension component of the load-line displacement (d_{11t}/L) and an uncracked ligament length (b/W) dependent parameter η_{pr} as

$$\eta_p = \eta_{pr}\, f(d_{11t}/L) \qquad (11)$$

For bending case $f(d_{11}/L)$ becomes unity and $\eta_p = \eta_{pr}$.

Assuming that the average tensile strain $\epsilon_n = d_{11t}/L$ is proportional to the strain at the midsection of the uncracked ligament (b), d_{11t}/L may be expressed in terms of the load-line displacement d_{11}/L (average strain at the load-line section) derived using similar triangles as shown in the Figure 7. Since the similar triangle relationship is not exact, a geometry dependent term b/W, with an unknown exponent m, is also

introduced. Therefore,

$$d_{11t}/L = \epsilon_n = \beta \ (d_{11}/L) \ (b/W)^m \qquad (12)$$

where

$$\beta = \frac{b/W \ (2\alpha - 1)}{(1 - 2(1 - \alpha) \ b/W)} \qquad (13)$$

The exponent m will be evaluated later. The value of β varies between 0 for $b/W = 0$ (pure bending) and 1 for $b/W = 1$ (pure tension). Equation 12 gives the average tensile strain (ϵ_n) between the gage points in the specimen. This strain component can be related to the material stress-strain curve through the secant modulus (E_s) as shown in the Figure 1(b). Therefore, η_p in Eq. 11 is expressed in terms of the normalized secant modulus (E_s/E), to account for the tensile component of the displacement by replacing $f(d_{11t}/L)$ as follows

$$\eta_p = \eta_{pr} \ (E_s/E)^n \qquad (14)$$

The exponent n will be evaluated later. As mentioned previously, the secant modulus is obtained from the ϵ_n given by Eq. 12. The unknowns to be evaluated for computing η_p are m, n, and η_{pr}. Note that m and n in Eqs. 12 and 14 are constants and they should be independent of crack length. In a nonlinear problem, like the present example, unless correct kinematic forms are selected for Eqs. 12 and 14 there is no guarantee that unique

values of m and n can be found which are valid for all crack geometries. The constants m, n, and η_{pr} were evaluated by using the values of J and J_p ($J_p = (J - J_e)_{EDI}$) from the EDI method. Substituting for J_p in Eq. 9, η_p can be calculated from

$$\eta_p = \frac{(J - J_e)_{EDI}\ b\ B}{\int P\ d\ (d_{11p})} \qquad (15)$$

The denominator represents the total plastic energy calculated from the area under the load P versus plastic load-line displacement curve. η_p was calculated for each crack length and at every increment of applied displacement. Then at each of the η_p, η_{pr} was calculated from Eq. 14 using the average tensile strain ϵ_n (Eq. 12), material stress-strain data (Fig. 1(b)) to define E_s/E, and by using different trial values for m and n. Variations of η_{pr} with d_{11} were examined for each pair of m and n for all a/W ratios. The values of m and n which gave nearly constant η_{pr} (within ± 5% variation) for each a/W and at all d_{11} (larger than twice the initial elastic displacement) were selected. In this numerical parametric study, the selection of m and n was simplified because it was found that m influenced the transition of deformation from tension to bending and n influenced the shape of the J curve at small a/W ratios. Value of m = 2 and n = 1/2 was found to fit results

for all crack lengths. Therefore, Eqs. 12 and 14 are written as

$$d_{11t}/L = \epsilon_n = \beta \ (d_{11}/L) \ (b/W)^2 \qquad (16)$$

and

$$\eta_p = \eta_{pr} \sqrt{(E_s/E)} \qquad (17)$$

Values of η_{pr} for different a/W ratios are given in Table 1 and are shown as the symbols in the Figure 9. Note that $b/W = 0$ represent the limiting condition of a pure bending problem, for which $\beta = 0$, $d_{11t}/L = 0$, and $\eta_p = \eta_{pr} = \eta'_p = 2$ [1]. The pure bending solution is shown by a solid symbol in the Figure 9.

Table 1. η_{pr} for various a/W ratios.

a/W	0.5	0.4	0.3	0.2	0.1	0.05
η_{pr}	2.2	2.0	1.85	1.55	0.66	0.25

The solid line in Figure 9 is a best fit to the η_{pr} values in Table 1 and the limiting value of 2 at $a/W = 1$. The equation for this best fit line is

$$\eta_{pr} = 2.52 - 0.52 \ (a/W) - 2.90 \ (b/W)^5 \qquad (18)$$

This equation approaches the Clarke and Landes [3] equation for deeply cracked compact specimens (see Fig. 9).

The J-values calculated from the η_p-factor method (referred to as J_{eq} in Fig. 7) are compared with the J-values from the EDI method in the Figure 7 for various a/W ratios. The two results agree well with each other for all four a/W ratios. Note that the results from J_{eq} were nearly identical to J_{EDI} for a/W = 0.5. Results for an a/W = 0.3 showed the largest difference between J_{EDI} and J_{Eq}, which was about ten percent.

7. CONCLUDING REMARKS

Three dimensional, elastic-plastic, finite-element analyses of single-edge-crack tension, SE(T), specimens for a wide range of crack-length-to-width ($0.05 \leq a/W \leq 0.5$) ratios were performed. The material was A36 steel and the stress-strain curve was represented by a piecewise linear approximation. The J-integral along the crack front was evaluated using the equivalent domain integral method. The analysis used small strain theory, the von Mises yield criterion, and the associated flow theory. The following conclusions were made from this study:

1. The material stress-strain curve (for example, the initial yield plateau) needs to be accurately modelled for shallow cracks ($a/W \leq 0.3$) to predict all characteristics (for example, the sharp knee) of the load against load-line displacement curves.
2. At large plastic deformations, both the total and the

plastic components of crack-tip-opening displacements are linearly proportional to the respective crack-mouth-opening displacements.

3. A deformation dependent plastic eta-factor (η_p) was developed for SE(T) specimens. η_p is valid for the complete range of crack-length-to-width ratios considered. η_p is a function of crack length and the secant modulus of the material corresponding to the tension component of the load-line displacement. J-values from the η_p method agreed well with those from the EDI method. The deformation dependent η_p is developed for A36 steel and further research was needed to generalize to all other materials.

REFERENCES

1. RICE, J. R., PARIS, P. C., and MERKLE, J. G. - In progress in flaw growth and fracture toughness testing. ASTM STP 536, American Society for Testing and Materials, pp. 231-245, 1973.

2. PARIS, P. C., ERNST, H. A., and TURNER, C. E. - A J integral approach to development of η-factors. Fracture mechanics: Twelfth conference ASTM STP 700, American Society for Testing and Materials, pp. 338-351, 1980.

3. CLARKE, G. A. and LANDES, J. D. - J. Testing and Evaluation, Vol. 7, No. 5, pp. 264-269, 1979.

4. MERKLE, J. G. and CORTEN, H. T. - A J integral analysis for the compact specimen. Trans. ASME, J. Pressures Vessel and Tech., Vol. 96, No. 4, pp.286-292, 1974.

5. ERNST, H. A. - Unified solution for J ranging continuously from pure bending to pure tension. Fracture Mechanics: Fourteenth Symposium - Volume I: Theory and Analysis, ASTM STP 791, J. C. Lewis and G sines, Eds., American Society for Testing and Materials, pp. I-499 - I-519, 1983.

6. TURNER, C. E. - The ubiquitous η factor. Fracture mechanics: Twelfth conference ASTM STP 700, American Society for Testing and Materials, pp. 314-337, 1980.

7. NIKISHKOV, G. P. and ATLURI, S. N. - Calculation of fracture mechanics parameters for an arbitrary three-dimensional crack, by the 'equivalent domain integral' method. Int. J. Numer. Methods in Engng., Vol. 24, pp. 1801-1821, 1987.

8. MORAN, B. and SHIH, C. F. - Crack tip and associated domain integrals from momentum and energy balance. Engng. Fract. Mech., Vol. 27, pp. 615-642, 1987.

9. SHIVAKUMAR, K. N. and RAJU, I. S. - A three dimensional equivalent domain integral for mixed mode fracture problems. NASA CR-182021, 1990.

10. TRACEY, D. M. - Finite-element solutions for crack-tip behavior in small-scale yielding. Trans. ASME, J. Engng. Materials and Technology, Vol. 98, pp. 140-151, 1976.

11. CHERMAHINI, R. G., SHIVAKUMAR, K. N., and NEWMAN Jr., J. C. - Three-dimensional finite-element simulation of fatigue-crack growth and closure. Mechanisms of Fatigue Crack Closure: ASTM STP 982, American Society for Testing and Materials, 1988.

12. CHERAPANOV, G. P. - Mechanics of Brittle Fracture, Translated and edited by R. W. De Wit and W. C. Cooly, McGraw Hill, New York, 1979.

13. de LORENZI, H. G. - On energy release rate and the J-integral for 3-D crack configuration. Int. J. Fracture, Vol. 19, pp. 183-192, 1982.

14. SIH, G. C. - A review of the three-dimensional stress problem for a cracked plate. Int. J. Fracture Mechanics, Vol. 7, pp. 39-61, 1971.

15. SHIVAKUMAR, K. N. and RAJU, I. S. - Treatment of singularities in cracked bodies. NASA CR-181840, 1989.

16. CREWS Jr., J. H, SHIVAKUMAR, K. N., and RAJU, I. S. - Effects of anticlastic curvature on G distributions for DCB specimens. 30th AIAA/ASME/ASCE/AHS Structures, Structural Dynamics, and Materials Conference, Paper AIAA-89-1300, Mobile, Alabama, April 3-5, 1989.

17. TADA, H., PARIS, P. C., and IRWIN, G. R. - The stress analysis of cracks handbook, Del Research Corp., St. Louis, 1973.

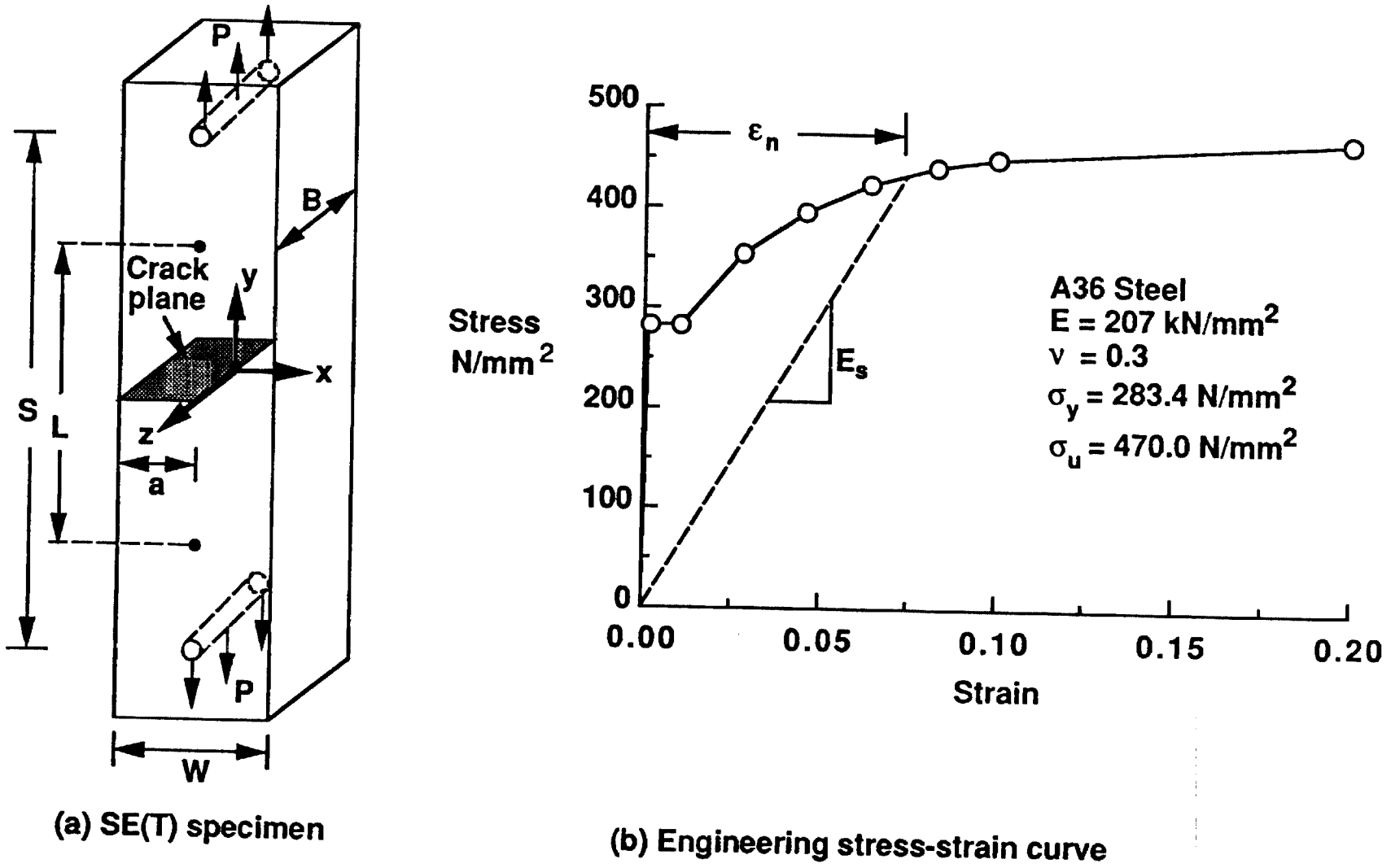

(a) SE(T) specimen

(b) Engineering stress-strain curve

Figure 1.- Specimen configuration and stress-strain curve.

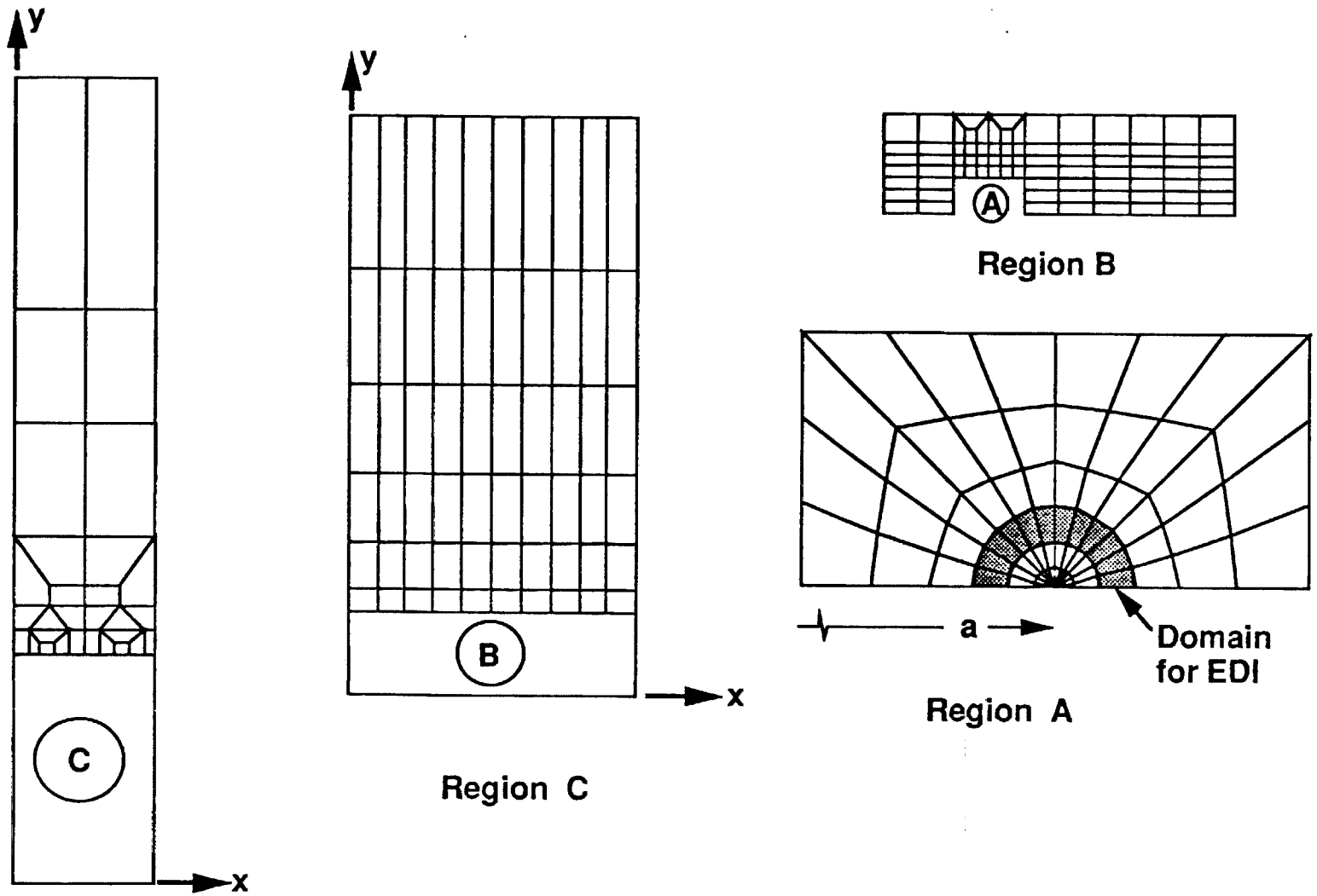

Figure 2.- Finite-element idealization of a SE(T) specimen at z=0 plane (a/W = 0.3).

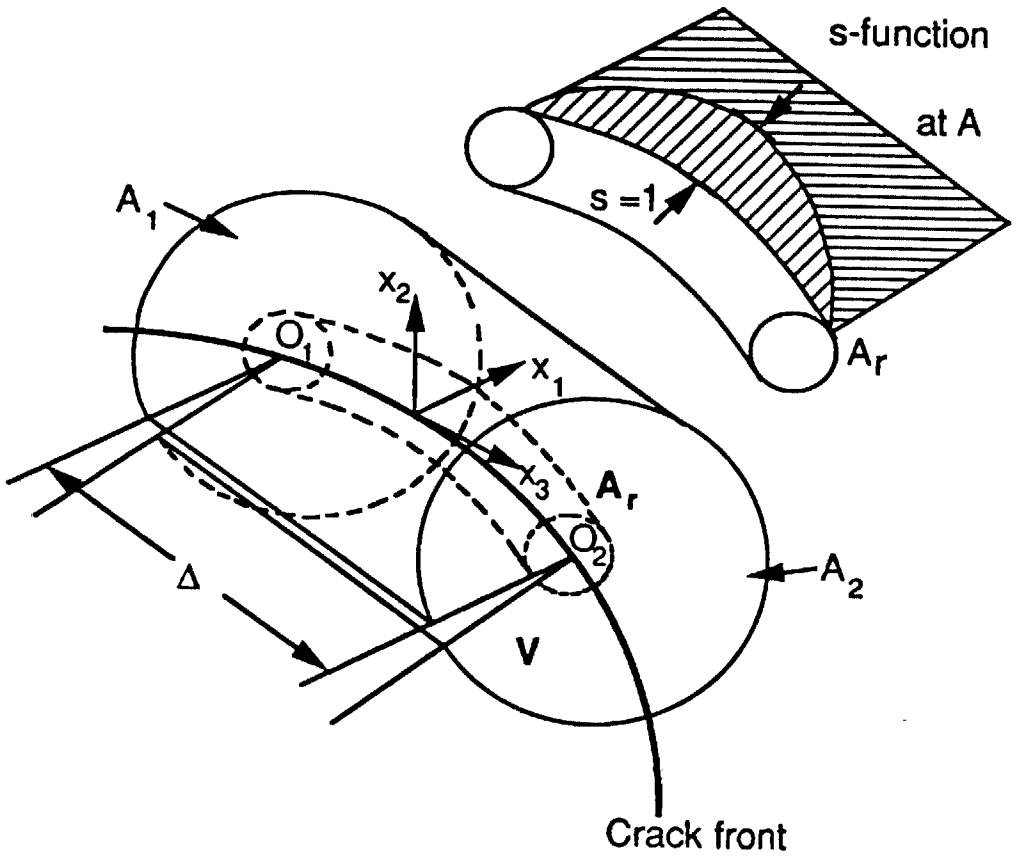

Figure 3.- Domain around the crack front

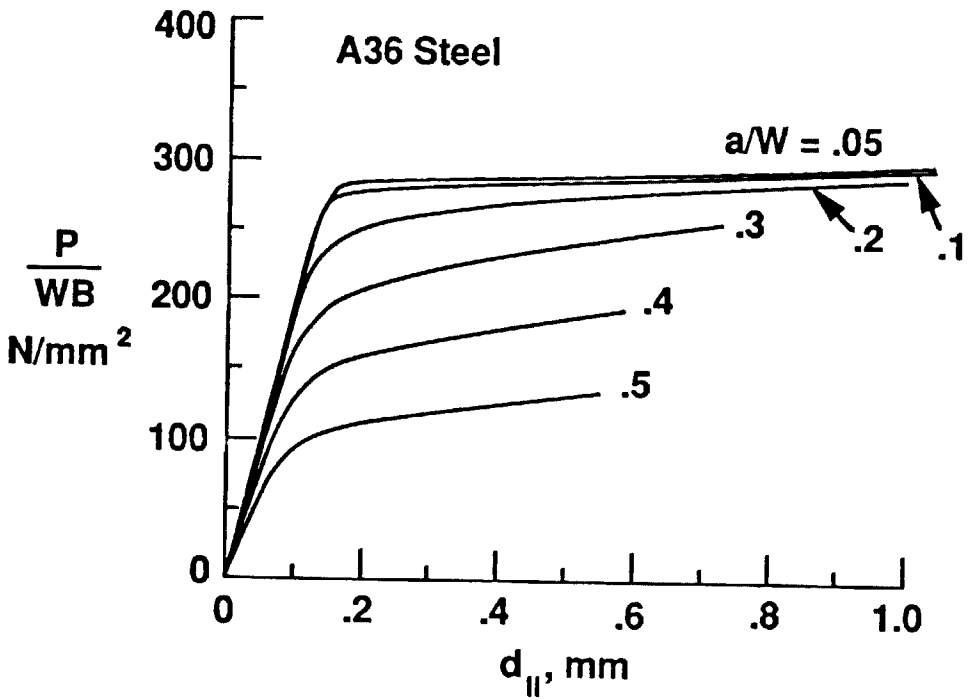

Figure 4.- Normalized load against load-line displacement for various a/W ratios.

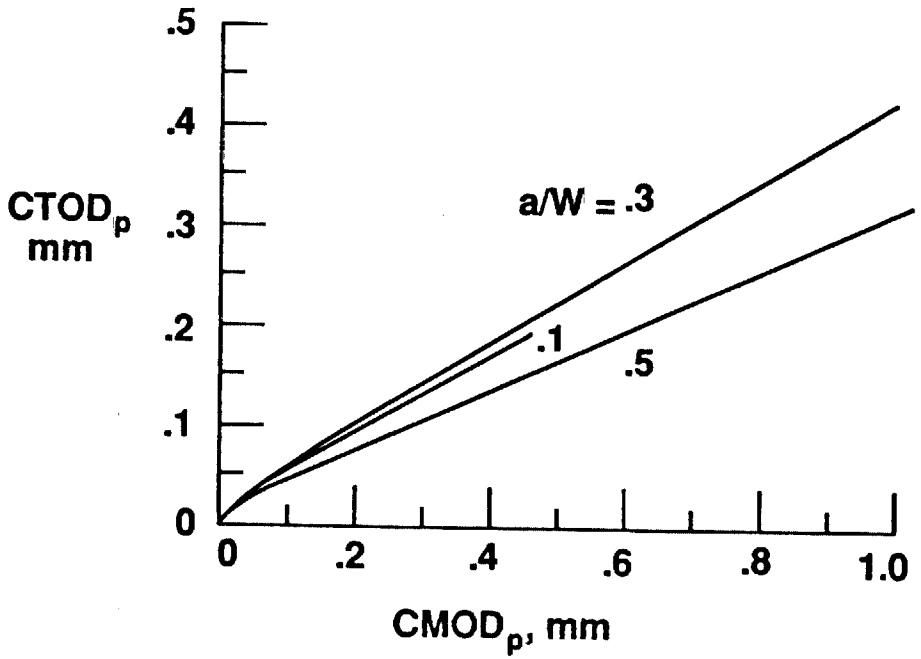

Figure 5.- Plastic component of CTOD against CMOD from 90 degree intercept method[10].

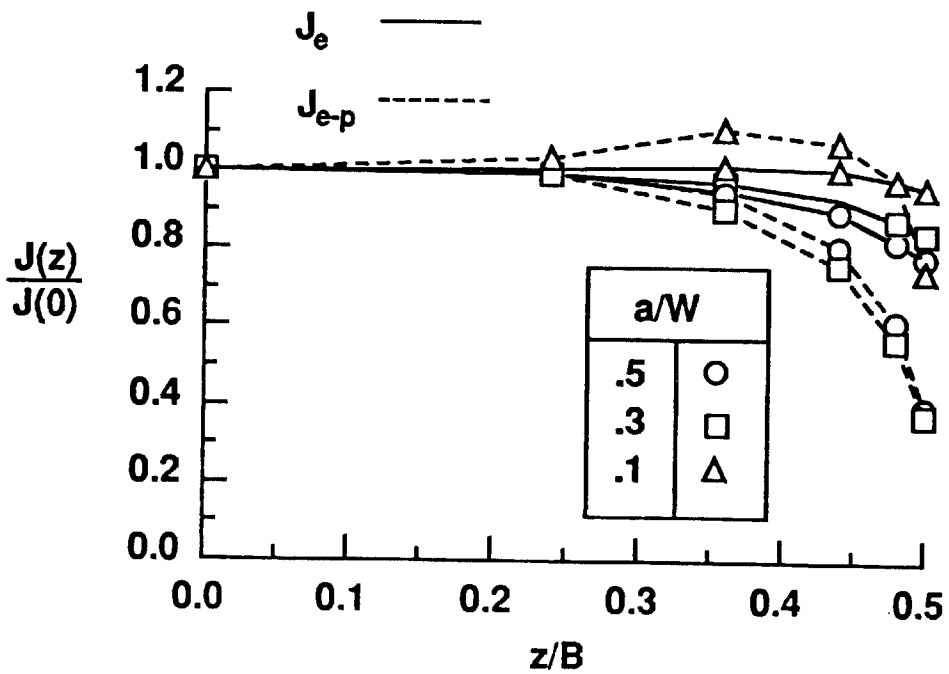

Figure 6.- Normalized J distribution along the crack front for various a/W ratios.

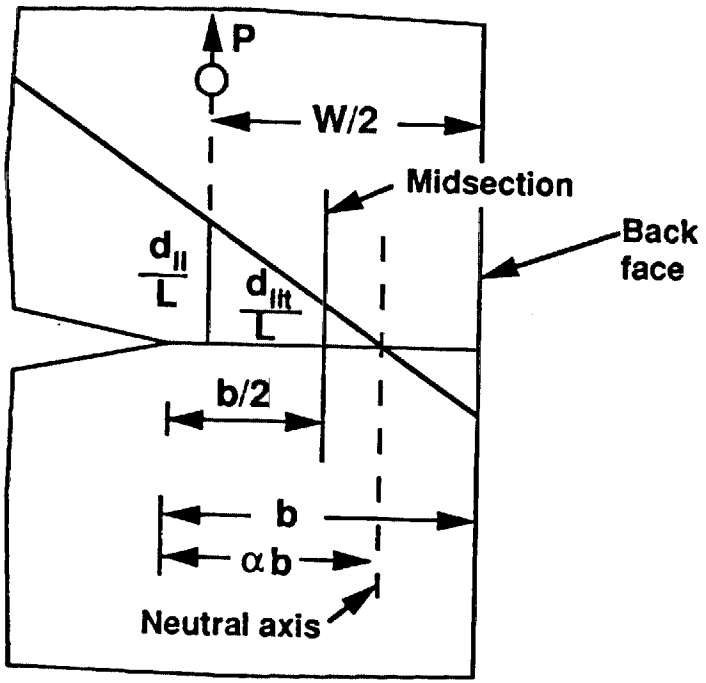

Figure 7.- Displacement diagram for a ligament subjected to tension-bending laoding.

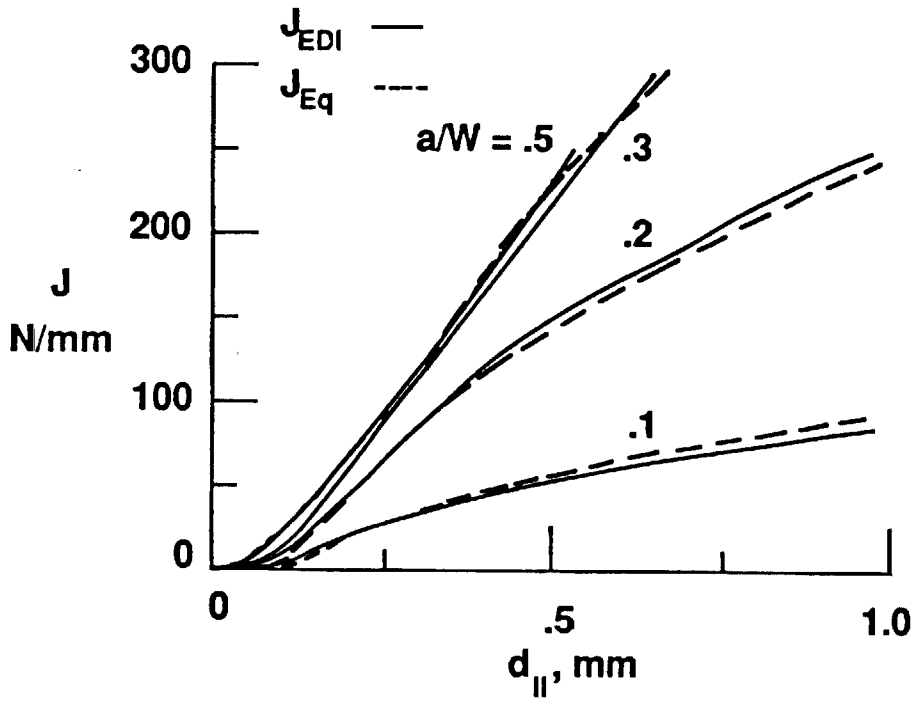

Figure 8.- J against load-line displacement for various a/W ratios.

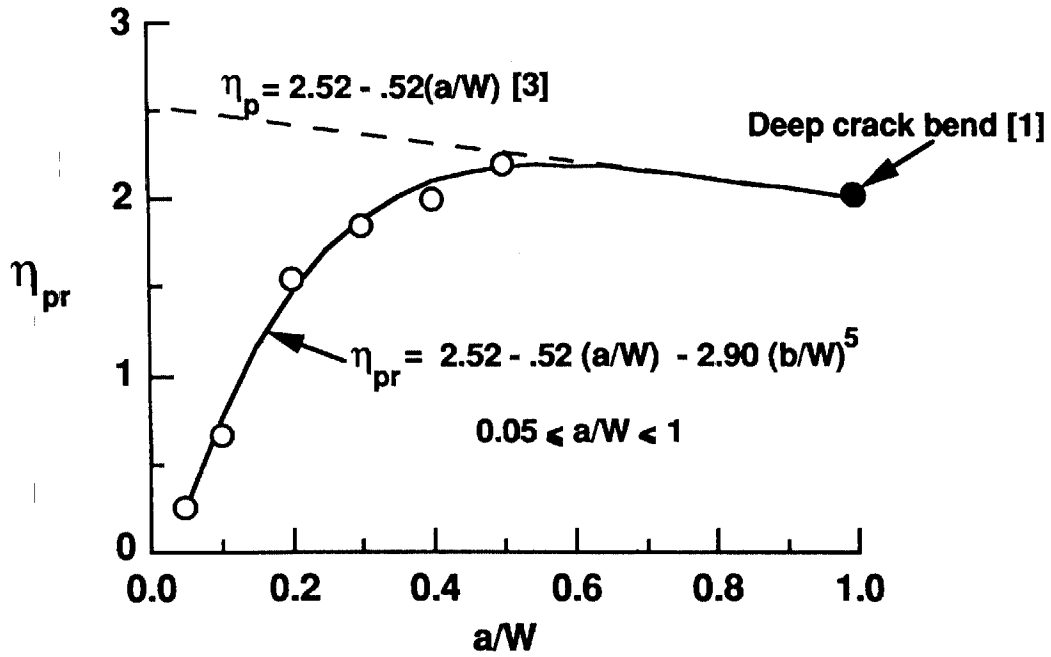

Figure 9.-Variation of η_{pr} with crack-length-to-width ratio.

NASA
National Aeronautics and Space Administration

Report Documentation Page

1. Report No.	2. Government Accession No.	3. Recipient's Catalog No.
NASA TM-102636		

4. Title and Subtitle

Three-Dimensional Elastic-Plastic Analysis of Shallow Cracks in Single-Edge-Crack-Tension Specimens

5. Report Date

April 1990

6. Performing Organization Code

7. Author(s)

Kunigal N. Shivakumar*
James C. Newman, Jr.

8. Performing Organization Report No.

10. Work Unit No.

505-63-01-05

9. Performing Organization Name and Address

NASA Langley Research Center
Hampton, VA 23665-5225

11. Contract or Grant No.

13. Type of Report and Period Covered

Technical Memorandum

12. Sponsoring Agency Name and Address

National Aeronautics and Space Administration
Washington, DC 20546-0001

14. Sponsoring Agency Code

15. Supplementary Notes

*Analytical Services and Materials, Inc., Hampton, VA

16. Abstract

Three-dimensional, elastic-plastic, finite-element results are presented for single-edge-crack-tension specimens with several shallow crack-length-to-width ratios ($0.05 \leq a/W \leq 0.5$). Results showed the need to model the initial yield plateau in the stress-strain behavior to accurately model deformation of the A36 steel specimens. The crack-tip-opening-displacement was found to be linearly proportional to the crack-mouth-opening displacement. A new deformation dependent η_{tp} (plastic-eta factor) equation is presented for calculating the J-integral from test load-displacement records. This equation was shown to be accurate for all crack lengths considered.

17. Key Words (Suggested by Author(s))	18. Distribution Statement
Three-dimensional analysis finite-element method elastic-plastic analysis single-edge-crack-tension specimen J-integral	Unclassified - Unlimited Subject Category - 24

19. Security Classif. (of this report)	20. Security Classif. (of this page)	21. No. of pages	22. Price
Unclassified	Unclassified	31	A03